Diode-pumped passively Q-switched Nd:YVO$_4$ laser with GaAs saturable absorber

Guiqiu Li (李桂秋), Shengzhi Zhao (赵圣之), Kejian Yang (杨克建), and Hongming Zhao (赵宏明)

School of Information Science and Engineering, Shandong University, Ji'nan 250100

The intracavity photon density is assumed to be of Gaussian spatial distributions and its longitudinal variation is also considered in the rate equations for a laser diode (LD) end-pumped passively Q-switched Nd:YVO$_4$ laser with GaAs saturable absorber. These space-dependent rate equations are solved numerically. The dependences of pulse width, pulse repetition rate, single-pulse energy, and peak power on incident pump power are obtained. In the experiment, the LD end-pumped passively Q-switched Nd:YVO$_4$ laser with GaAs saturable absorber is realized and the experimental results are consistent with the numerical solutions.

OCIS codes: 140.3430, 140.3480, 140.3540, 140.3580.

In recent years, laser diode (LD) pumped solid-state Q-switched lasers have attracted a great deal of attention. All solid-state Q-switched lasers have wide applications in the fields of remote sensing, information storage, coherent telecommunications, medicine, etc.. Compared with actively Q-switched lasers, the passively Q-switched lasers have the advantages of simplicity, compactness, high efficiency, and low cost. Passive Q-switching technique is usually accomplished with intracavity saturable elements such as dyes, Cr^{4+}:YAG, and semiconductors. Semiconductor saturable absorber GaAs has become another attractive candidate for passive Q-switchs due to the large optical nonlinearity[1−7]. GaAs wafer working as saturable absorber as well as output coupler has been often reported[1−6]. But GaAs wafer working as passive Q-switch and middle mirror has been seldom reported[7]. Rate equations are efficient tools for analyzing the performance of the Q-switched laser. However, the rate equations in Refs. [5−7] are obtained under a plane-wave approximation. For the LD-pumped passively Q-switched laser, this assumption is not properly satisfied because the intracavity photon density should be of the Gaussian distribution. When the Gaussian distribution of the intracavity photon density is taken into account in the rate equations, the theoretical results obtained by numerically solving these rate equations are more close to the experimental results than those obtained under the plane-wave approximation[8,9]. Therefore, for a more accurate and general theoretical analysis of the pulses from the LD-pumped passively Q-switched laser with GaAs saturable absorber, it is desirable to consider the transversal distribution and longitudinal variation of the intracavity photon density in the rate equations.

The experimental setup is depicted in Fig. 1, in which Nd:YVO$_4$ works as the gain medium and GaAs works as the passive Q-switch. If the intracavity photon density is assumed to be of the Gaussian spatial distribution during the entire formatting process of the LD-pumped passively Q-switched laser pulse, the intracavity photon density for the TEM$_{00}$ mode can be expressed as

$$\phi(r,t) = \phi(0,t)\exp\left(-\frac{2r^2}{w_l^2}\right), \qquad (1)$$

where r is the radial coordinate, w_l is the average radius of the TEM$_{00}$ mode, which is mainly determined by the geometry of the resonator, and $\phi(0,t)$ is the photon density in the laser axis. The photon densities $\phi_g(r,t)$ and $\phi_s(r,t)$ at the two positions of Nd:YVO$_4$ crystal and saturable absorber can be expressed as[10]

$$\phi_g(r,t) = \frac{w_l^2}{w_g^2}\phi(0,t)\exp\left(-\frac{2r^2}{w_g^2}\right), \qquad (2)$$

$$\phi_s(r,t) = \frac{w_l^2}{w_s^2}\phi(0,t)\exp\left(-\frac{2r^2}{w_s^2}\right), \qquad (3)$$

where w_g and w_s are the radii of the TEM$_{00}$ mode at the above mentioned two positions, respectively.

So for this laser, if the Cr^{4+}:YAG saturable absorber is near the output mirror and only considering single-photon absorption (SPA) and two-photon absorption (TPA), we can obtain the coupling rate equations[10−12]

$$\int_0^\infty \frac{d\phi(r,t)}{dt}2\pi r dr = \int_0^\infty \frac{1}{t_r}\{2\sigma n(r,t)l\phi_g(r,t)$$

$$-2\sigma^+ n^+(r,t)l_s\phi_s(r,t) - 2\sigma^0[n_0 - n^+(r,t)]l_s\phi_s(r,t)$$

$$-Bl_s\phi_s^2(r,t) - \ln\left(\frac{1}{R}\right)\phi_s(r,t) - L\phi(r,t)\}2\pi r dr, \qquad (4)$$

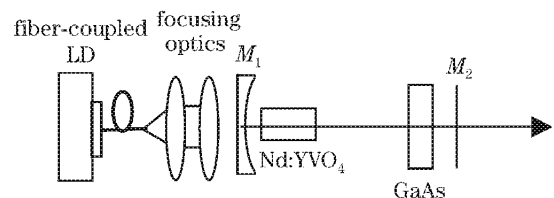$$\frac{dn(r,t)}{dt} = f_a R_{in}(r) - (f_a + f_b)\sigma c n(r,t)\phi_g(r,t) - \frac{n(r,t)}{\tau}, \qquad (5)$$

Fig. 1. Schematic of the experimental setup.

$$\frac{\mathrm{d}n^+(r,t)}{\mathrm{d}t} = c\phi_s(r,t)\{\sigma^0[n_0 - n^+(r,t)] - \sigma^+ n^+(r,t)\},$$

(6)

where $n(r,t)$ is the average population-inversion density; n_0 is the total population density of the EL2 defect level (including EL2^0 and EL2$^+$) of GaAs saturable absorber; $n^+(r,t)$ is the population density of positively charged EL2$^+$; σ and l are the stimulated-emission cross section and length of Nd:YVO$_4$ gain medium, respectively; σ^0 and σ^+ are the absorption cross sections of EL2^0 and EL2$^+$, respectively; l_s is the length of the saturable absorber; t_r is the round-trip time of light in the resonator $\{t_r = [2n_1 l + 2n_2 l_s + 2(L_e - l - l_s)]/c\}$, n_1 and n_2 are the refractive indices of Nd:YVO$_4$ gain medium and GaAs saturable absorber, respectively, L_e is the cavity length, c is the velocity of light in vacuum; $B = 6\beta h\gamma c(w_g/w_s)^2$ is the coupling coefficient of TPA in GaAs, where β is the absorption coefficient of two photons, $h\gamma$ is the single photon energy of the fundamental wave[5]; R is the reflectivity of the output mirror; L is the intrinsic loss; f_a and f_b are the Boltzman occupation fractions of the upper and lower levels, respectively; τ is the stimulated-radiation lifetime of the gain medium; $R_{\mathrm{in}}(r) = P_{\mathrm{in}}[1 - \exp(-\alpha l)]\exp(-2r^2/w_p^2)/h\gamma_p\pi w_p^2 l$ is the pump rate, where P_{in} is the pump power, $h\gamma_p$ is the single photon energy of the pump light, w_p is the average radius of the pump beam, α is the absorption coefficient of the gain medium.

The initial conditions of Eqs. (5) and (6) can be written as[10]

$$n^+(r,0) = n^+,$$

(7)

$$n(r,0) = n(0,0)\exp\left(-\frac{2r^2}{w_p^2}\right),$$

(8)

where n^+ is the initial population density of positively charged EL2$^+$ of GaAs saturable absorber, $n(0,0)$ is the initial population-inversion density in the laser axis, i.e.

$$n(0,0) = \frac{\ln\left(\frac{1}{T_0^2}\right) + L + \ln\left(\frac{1}{R}\right)}{2\sigma l}\left(1 + \frac{w_g^2}{w_p^2}\right),$$

(9)

where $T_0 = \exp\{-[\sigma^0(n_0 - n^+) + \sigma^+ n^+]l_s\}$ is the small-signal transmission of the saturable absorber.

Substituting Eqs. (2), (3), (7), and (8) into Eqs. (5) and (6) and integrating the results over time, we obtain

$$n(r,t) = \exp\left[-(f_a + f_b)\sigma c\frac{w_l^2}{w_g^2}\exp\left(-\frac{2r^2}{w_g^2}\right)\right.$$

$$\times \int_0^t \phi(0,t)\mathrm{d}t - \frac{t}{\tau}\right]$$

$$\times \left\{f_a R_{\mathrm{in}}(r)\int_0^t \exp\left[(f_a + f_b)\sigma c\frac{w_l^2}{w_g^2}\exp\left(-\frac{2r^2}{w_g^2}\right)\right.\right.$$

$$\left.\times \int_0^t \phi(0,t)\mathrm{d}t + \frac{t}{\tau}\right]\mathrm{d}t + n(0,0)\exp\left(-\frac{2r^2}{w_p^2}\right)\right\}, \quad (10)$$

$$n^+(r,t) = \exp\left[-c(\sigma^0 + \sigma^+)\frac{w_l^2}{w_s^2}\exp\left(-\frac{2r^2}{w_s^2}\right)\int_0^t \phi(0,t)\mathrm{d}t\right]$$

$$\times \left\{c\sigma^0 n_0\frac{w_l^2}{w_s^2}\exp\left(-\frac{2r^2}{w_s^2}\right)\int_0^t \phi(0,t)\right.$$

$$\times \exp\left[c(\sigma^0 + \sigma^+)\frac{w_l^2}{w_s^2}\exp\left(-\frac{2r^2}{w_s^2}\right)\int_0^t \phi(0,t)\mathrm{d}t\right]\mathrm{d}t + n^+\right\}.$$

(11)

Substituting Eqs. (1)–(3) into Eq. (4), we obtain

$$\frac{\mathrm{d}\phi(0,t)}{\mathrm{d}t} = \frac{4\phi(0,t)}{w_l^2 t_r}\int_0^\infty \left\{2\sigma n(r,t)l\frac{w_l^2}{w_g^2}\exp\left(-\frac{2r^2}{w_g^2}\right)\right.$$

$$-2\sigma^+ n^+(r,t)l_s\frac{w_l^2}{w_s^2}\exp\left(-\frac{2r^2}{w_s^2}\right)$$

$$-2\sigma^0[n_0 - n^+(r,t)]l_s\frac{w_l^2}{w_s^2}\exp\left(-\frac{2r^2}{w_s^2}\right)$$

$$-Bl_s\phi(0,t)\frac{w_l^4}{w_s^4}\exp\left(-\frac{4r^2}{w_s^2}\right)$$

$$-\ln\left(\frac{1}{R}\right)\frac{w_l^2}{w_s^2}\exp\left(-\frac{2r^2}{w_s^2}\right) - L\exp\left(-\frac{2r^2}{w_l^2}\right)\right\}r\mathrm{d}r,$$

(12)

where $n(r,t)$ and $n^+(r,t)$ are given in Eqs. (10) and (11), respectively. Equation (12) is the basic differential equation describing $\phi(0,t)$ as a function of t. By numerically solving Eq. (12) and from Eq. (3), we can obtain the relation between $\phi_s(0,t)$ and t. Thus we can obtain the pulse width (full-width at half-maximum, FWHM) W and the pulse repetition rate F. According to the relationship of power and photon density, the pulse peak power P and the single-pulse energy E can be expressed as

$$P = \frac{1}{4}\pi w_s^2 h\gamma c\ln\left(\frac{1}{R}\right)\phi_{\mathrm{sm}},$$

(13)

$$E = PW,$$

(14)

where $h\gamma$ is the single photon energy of the fundamental wave, h is the Planck's constant, and ϕ_{sm} is the maximum value of $\phi_s(0,t)$.

The corresponding parameters values of the theoretical calculation are shown in Table 1[11,12]. Using the values in Table 1, we calculate that the small-signal transmission of the GaAs saturable absorber is $T_0 = 93.9\%$. The dotted line in Fig. 3 shows the theoretical pulse shape at $R = 90\%$ and a pump power of 3.77 W. The solid lines in Figs. 4–7 are the theoretical calculation curves for pulse width W, pulse repetition rate F, single-pulse energy E, and peak power P versus pump power, respectively.

In Fig. 1, the pump source is a fiber-coupled LD (FAP-I system Coherent Inc., USA) which works at the maximum absorption wavelength (808 nm) of the Nd:YVO$_4$ crystal. The mirror M_1 with 150-mm curvature radius

Table 1. Parameters of the Theoretical Calculation

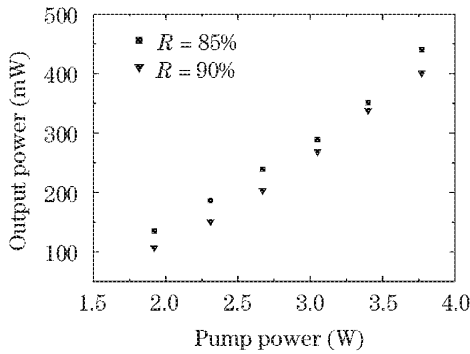| σ	3.42×10^{-18} cm^2	l_s	580 μm
σ^0	1.0×10^{-16} cm^2	l	0.5 cm
σ^+	2.3×10^{-17} cm^2	w_p	330 μm
n_0	1.2×10^{16} cm^{-3}	L	0.08
n^+	1.4×10^{15} cm^{-3}	α	5.32 cm^{-1}
τ	98 μs	w_g	233 μm
β	2.6×10^{-8} cmW^{-1}	w_s	159 μm
n_1	2.183	w_l	180 μm
n_2	3.48	f_a	0.48
L_e	8 cm	f_b	0.23

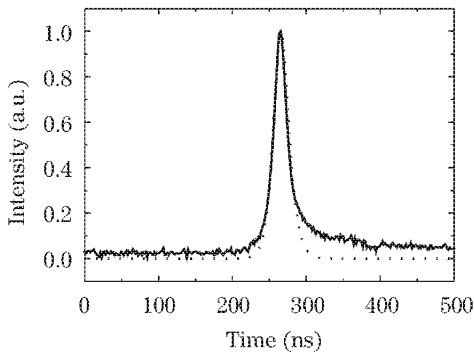Fig. 2. Average output power versus pump power.

Fig. 3. Temporal profile of single pulse with $R = 90\%$. Solid line: oscilloscope trace; dotted line: calculated result.
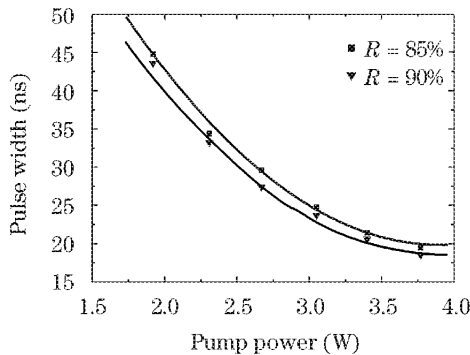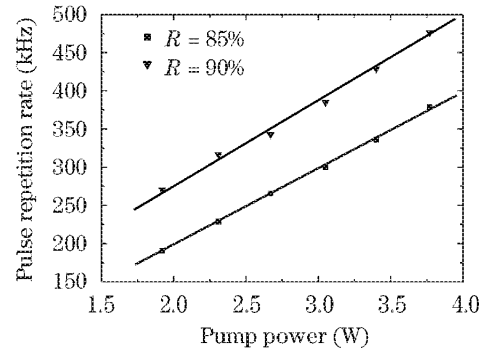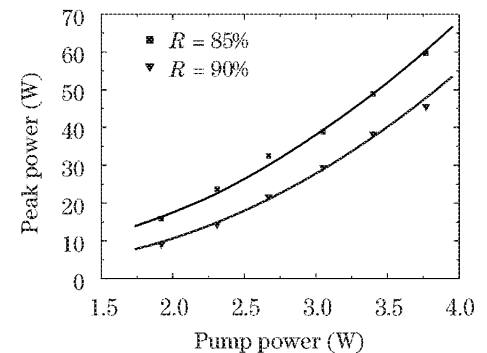

Fig. 4. Pulse width versus pump power.

is high antireflection coated at 808 nm and high reflection coated at 1064 nm. The Nd:YVO$_4$ crystal doped with

1.0 at.-% Nd^{3+} ions is $4 \times 4 \times 5$ mm^3 and its absorption coefficient at 808 nm is 5.32 cm^{-1}. Its first surface is antireflection coated at 808 nm and the other surface is high antireflection coated at 1064 nm. The temperature of the Nd:YVO$_4$ crystal is controlled at 20 °C by means of a temperature controller. The output mirror M_2 is a plane mirror. The reflectivities of the two output mirrors are $R = 85\%$ and $R = 90\%$, respectively. The distance between M_1 and M_2 is about 8 cm. So from the cavity configuration, we calculate that the radii of the Gaussian beam waists at two positions Nd:YVO$_4$ crystal and saturable absorber are 0.233 and 0.159 mm, respectively. The values of the two radii are given in Table 1. A LPE-1B power meter (Institute of Physics, Chinese Academy of Science) is used to measure the average output power and a TED620B digital oscilloscope (Tektronix Inc., USA) is used to measure the pulse width and the pulse repetition rate.

Fig. 5. Pulse repetition rate versus pump power.
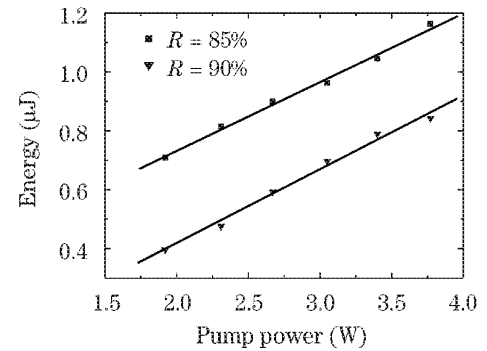
Fig. 6. Single-pulse energy versus pump power.

Fig. 7. Pulse peak power versus pump power.

Figure 2 shows the average output power P_A versus pump power. A single-pulse temporal profile of an oscilloscope trace at $R = 90\%$ and a pump power of 3.77 W is shown by the solid line in Fig. 3. The dependences of pulse width W and pulse repetition rate F on pump power are shown by scattered dots in Figs. 4 and 5, respectively. Using the equations $E = P_A/F$ and $P = E/W$, we obtain the single-pulse energy E and the peak power P versus pump power, which are shown by scattered dots in Figs. 6 and 7, respectively. From Figs. 3–7, we can see that the experimental results are in agreement with the theoretical calculations.

In conclusion, we have assumed the intracavity photon density to be of Gaussian spatial distributions and considered the longitudinal variation of the intracavity photon density in the rate equations for the LD end-pumped passively Q-switched Nd:YVO$_4$ laser with GaAs saturable absorber. These space-dependent rate equations are solved numerically. From the numerical solutions, we obtain the dependences of pulse width, pulse repetition rate, single-pulse energy, and peak power on pump power. The theoretical calculations of the numerical solutions agree with the experimental results obtained from the LD end-pumped passively Q-switched Nd:YVO$_4$ laser with GaAs saturable absorber.

References

1. T. T. Kajava and A. L. Gaeta, Opt. Lett. **21**, 1244 (1996).
2. D. Shen, D. Tang, and J. Kong, Opt. Commun. **211**, 271 (2002).
3. Q. Zhang, B. Feng, D. Zhang, P. Fu, Z. Zhang, Z. Zhao, P. Deng, J. Xu, X. Xu, Y. Wang, and X. Ma, Opt. Commun. **232**, 353 (2004).
4. P. Li, Q. Wang, S. Li, J. Lian, B. Ma, and J. He, Chin. Opt. Lett. **1**, 31 (2003).
5. J. Gu, F. Zhou, W. Xie, S. C. Tam, and Y. L. Lam, Opt. Commun. **165**, 245 (1999).
6. Q. Liu, M. Gong, P. Yan, W. Jia, R. Cui, and D. Wang, Acta Phys. Sin. (in Chinese) **51**, 2756 (2002).
7. P. Li, Q. Wang, X. Zhang, S. Zhao, Y. Wang, J. Wang, B. Huang, S. Zhang, X. Liu, J. He, and X. Lu, Acta Opt. Sin. (in Chinese) **22**, 298 (2002).
8. Q. Zhang, Q. Wang, X. Zhang, and S. Zhao, Laser Journal (in Chinese) **21**, 25 (2000).
9. X. Zhang, S. Zhao, and Q. Wang, Acta Photon. Sin. (in Chinese) **28**, 651 (1999).
10. G. Li, S. Zhao, H. Zhao, K. Yang, and S. Ding, Opt. Commun. **234**, 321 (2004).
11. J. Zheng, S. Zhao, and L. Chen, Opt. Eng. **41**, 2271 (2002).
12. L. Chen, S. Zhao, and H. Zhao, Opt. Laser Technol. **35**, 563 (2003).